Yang *et al. Carbon Research* (2024) 3:46
https://doi.org/10.1007/s44246-024-00127-y

Carbon Research

ORIGINAL ARTICLE

Open Access

Anthropogenic soil as an environmental material, as exemplified with improved growth of rice seedlings

Fan Yang[1,2*†], Yibo Lan[1,2†], Ronghui Li[1,2], Qiang Fu[1,2], Kui Cheng[1,3], Zhuqing Liu[1,2*] and Markus Antonietti[4*]

Abstract

Herein, the feasibility of artificial black soil (ABS) derived from hydrothermal humification-hydrothermal carbonization (HTH-HTC) for restructuration of weak soil was verified. This study breaks through the long history of soil formation and evolution, and obtains reconstructed anthropogenic soil (AS) system which only takes one month, for the further application of rice seedlings. HTH-HTC derived by-products are slightly acidic, which facilitates the effective nutrient uptake and prevention of wilt diseases for acid-loving rice seedlings. AS mainly consists of the inherent components retained from weak soil such as SiO_2 and minerals, and exogenous components such as artificial humic substances and hydrochar, as introduced by hydrothermal humification processes. Results exhibit that AS has high contents of ammonium nitrogen, organic matter, organic carbon, and abundant porous structure for nutrient transport and water holding, especially, the community diversity and richness of microbial system gets the expected recovery and new beneficial bacteria (such as *Caballeronia calidae*) or fungi (such as *Humicola*) appear. Positive effects of AS on agronomic traits in rice seedlings are quantified. As a general result, this study supports the application of AS in sustainable agriculture, and provides a novel strategy to tackle the already-omnipresent land degradation by anthropogenic misuse and larger scale accidents.

Highlights

- Anthropogenic soil system was rapidly reconstructed through hydrothermal humification-hydrothermal carbonation technology.
- Anthropogenic soil possesses multiple components-structure properties for nutrient transport and water retention.
- Anthropogenic soil microbial systems recover and spread in 4 weeks.
- Anthropogenic soil provides acidic environment to biochemically promote rice seedling growth.

Handling Editor Fengchang Wu.

†Fan Yang and Yibo Lan contributed equally to this work.

*Correspondence:
Fan Yang
yangfan_neau@163.com
Zhuqing Liu
lzq@cau.edu.cn
Markus Antonietti
Markus.Antonietti@mpikg.mpg.de
Full list of author information is available at the end of the article

Keywords Anthropogenic soil, Artificial black soil, Optimization of soil mechanical structure, Recovery of biological function

Graphical Abstract

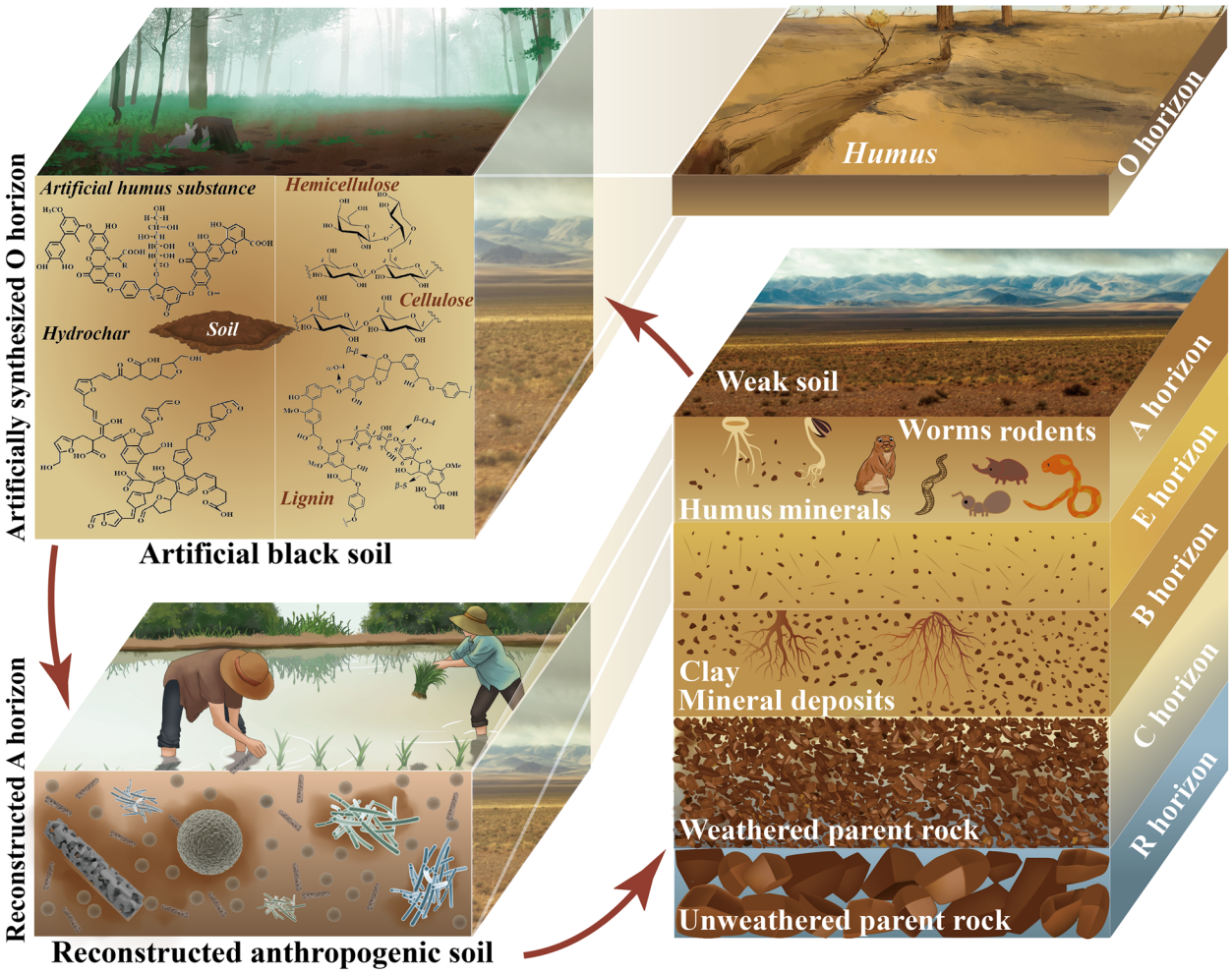

1 Introduction

Soil health is understood as the vitality for sustaining the socio-ecological functions of its enfolded land (Janzen et al. 2021). It is the essential measure of its "goodness" and suitability, quality and functionality, which is crucial for an operational ecosystem, water filtration, crop growth, and finally substantial carbon storage (Arcurs 2017). The climate discussion has often neglected the soil, which is the largest but often overlooked resource (Wall and Six 2015). One-third of the world's land surface is degraded to some degree, and 24 billion metric tons of fertile soil are lost each year (Coban et al. 2022). Soil degradation over about that in the next 20 years threatens to reduce global food productivity by 12% and to massively increase food prices (Kopittke et al. 2019).

Soil degradation has long term consequences, while rehabilitation requires short-term and low-cost measures (Richter 2021). Increasing humic substance through organic inputs is a historical measure for enhancing sustainable soil carbon storage and nutrient enrichment (Tautges et al. 2019). The artificial hydrogeochemical technique simulates humification for synthesizing artificial humic matter in a short time and with high carbon recovery rate (close to 1), providing a novel route for sustainable utilization of so called "waste-biomass" for the reconstruction of soil humus layer, and even laid the base

for the chemical retro-design and optimization of "black soils" (Yang et al. 2019b; Yang and Antonietti 2020). Furthermore, the rapid synthesis of environmental materials, namely anthropogenic soil as a "carbon pump", possess multiple functional component-structures and achieves 100% recycling of exogenous organic carbon, as compared to the previous individual components of artificial humic substances reported by our group (Yang et al. 2021a, 2023; Yang and Antonietti 2020).

While Matt Damon in the Hollywood blockbuster "The Martian" cleverly created "soil" in one day, the reality is that this would be extremely challenging (Wall and Six 2015; Arcurs 2017). Two viable short-term "soil generation" approaches are utilizing waste biomass and its derivatives (e.g., biogas digestate, sewage sludges, and biochar) mixed with other soil essential components for composting or hydrothermal carbonization. Such as seedling substrates made by composting different types of biogas residues, in which perlite and sawdust were used as additives in different proportions separately or together (Chang et al. 2021). However, apart from potential environmental risks (Yang et al. 2021a), Meng et al. demonstrated that corn straw biogas residue inhibited the growth of both tomatoes and peppers (Meng et al. 2022). And previous literature has demonstrated the phytotoxic effects of hydrochar, especially at the early stage of plants (Chen et al. 2022).

Herein, this study proposed an effective, in a first version necessarily bold engineering proposal to artificially re-construct a fertile soil system within 30 days, and the reconstitution was successfully tested by rice (*Oryza sativa* L.) seedling cultivation (Fig. 1). The major objectives are (i) to create a reinforced concentrated artificial black soil via hydrothermal humification—hydrothermal carbonization from biomass leftovers; (ii) to cultivate a natural microbiome system in anthropogenic soil through artificial black soil cultivation with natural weak soil; and (iii) to verify the adequacy of the dominant physical–chemical properties of anthropogenic soils, such as not requiring supplementary acid regulators and seedling strengtheners, and its agronomic performance in rice seedling. If successful, this describes and delineates a potential "cure for degraded farm land" starting from generating synthetic anthropogenic soil from waste biomass (or agricultural side products) and weak soil, potentially from the same or nearby farm-land.

2 Materials and methods

2.1 Experimental design

The hydrothermal humification—hydrothermal carbonization (HTH-HTC) technology is used to synthesize artificial black soil (ABS) for the reconstitution of weak farming soil. AS at the beginning mainly consisted of the inherent inorganic components retained from weak soil such as SiO_2 and minerals, and exogenous carbon components such as artificial humic substances and hydrochar were generated by the hydrothermal humification process and added to the minerals. The as-made chemical mixtures were then primed with a natural soil microbiome, and only after 4 weeks microbial colonialization had taken place to a much higher level, creating a living soil system.

2.2 Preparation of artifical black soil

Weak soil used in this study was obtained from Northeast Agriculture University in Harbin, China (45°44′22"N, 126°43′30"E) and lacked organic carbon. It was sampled in June 2022 at field capacity, which is approximately equivalent to a soil water potential of -100 hPa. Soil blocks were carefully retrieved from the 0–20 cm soil layer. The samples were air-dried, sieved (< 2 mm), and homogenized. Weak soil substance composition was provided in Table S1. The soil type in the US Soil Taxonomy was classified as Udic Argiboroll and was a clay loam. The annual mean temperature was 4 °C and the annual precipitation is 569 mm (Wang et al. 2018).

In total, 5 g weak soil and 2.5 g rice straw powders were added to KOH aqueous solution, and transferred to a 100 ml polytetrafluoroethylene-lined stainless steel autoclave, heated to 200 °C for 24 h. The liquid product (artificial fulvic acid, AFA) was stored at 4 °C in a light-proof environment for storage. The solid product (artificial black soil, ABS) was dried at 50 °C, ground until there were no visible lumps. The samples were named as ABS-20:1, ABS-15:1, and ABS-10:1 according to mass ratios of rice straw powder to KOH, and stored in a sealed dry environment. As the final pH was acidic, the samples were essentially biochar and articifical humic substances conjugated to the surface of the mineral grains. The control group was consisted of samples prepared without the addition of rice straw or KOH.

2.3 Functional rehabilitation of anthropogenic soil

Combining pH values of the above hydrothermal humification liquid products (different biomass to KOH ratios) presented in Table S2 and the characteristic that rice seedlings prefer acidic growth habitat, the ratio of biomass to KOH was set to be 15:1 for hydrothermal humification in the subsequent experiments, whereby artificial black soil used for the subsequent experiments was ABS-15:1 with high soil organic matter (SOM, 19.49 ± 1.40%) and soil organic carbon (SOC, 13.61 ± 1.18%) content, i.e., it is too carbon rich to be used as such. The novel artifical soil (AS) for rice seedling was thereby constructed through mixing various mass ratios of ABS-15 (0%, 10%, 30%, and 50%) with the original weak soil and

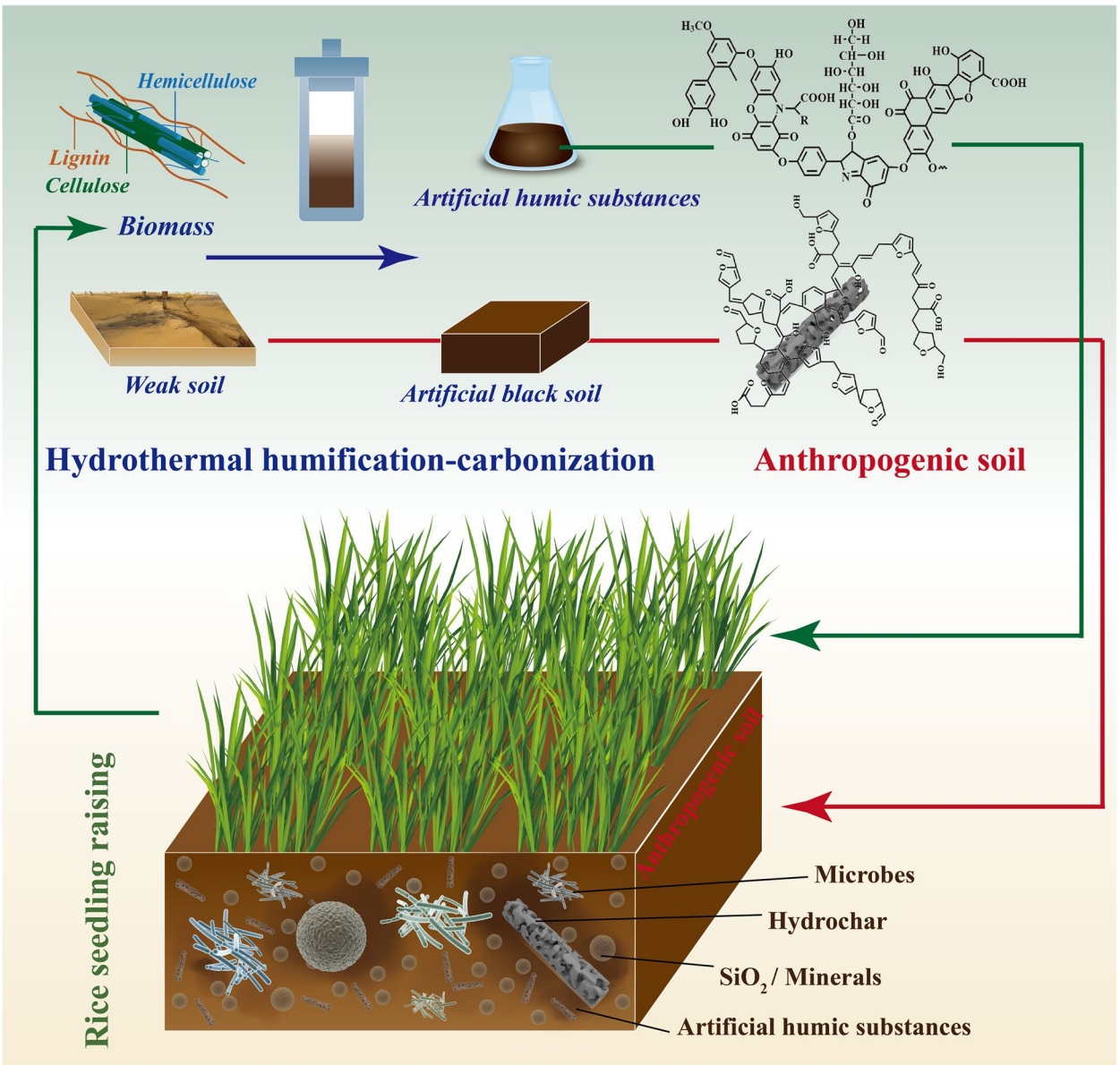

Fig. 1 Construction of anthropogenic soil using artificial humic substances derived from biomass for dilution on farmland back to promote the growth of biomass

sprayed with a certain amount of AFA (excluding the control group), named as CK, AS-10, AS-30, and AS-50, respectively, as shown in Table S3. The soil samples were then mellowed for almost 30 days to stimulate microbial growth.

Nutrient and functional indicators of AS were studied by quantitative tests of total organic matter, total organic carbon, available inorganic nitrogen (ammonium nitrogen, nitrate nitrogen), available phosphorus, bulk density (BD), and volumetric maximum water holding capacity (WHC). Fresh soil samples were extracted with 2 M KCl solution at a ratio of 1:10 (w/v), and the concentrations of ammonium (NH_4^+-N) and nitrate-nitrogen (NO_3^--N) in the extracts were tested with the Discrete Auto Analyzer (Smartchem200, Alliance, France). Available phosphorus was extracted with 0.5 M $NaHCO_3$ leaching at a ratio of 1:20 (w/v), and then were tested with the Discrete Auto Analyzer (Smartchem200, Alliance, France). Maximum WHC (aka "gravity-drained equilibrium water content" or "field-carrying capacity") and BD were determined in cylinders packed with soil or amended soil based on

the method of Veihmeyer and Hendrickson (1949) with some modifications following Verheijen et al. (2019).

The recovery degree of microbial communities in AS was visualized through high-throughput sequencing means. Amplification of 16S rRNA gene along with genomic DNA for DNA extraction, PCR amplification, high-throughput sequencing was done by using primer 16S rRNA 515F(5'-GTGCCAGCMGCCGCGG-3') and 907R(5'-CCGTCAATTCMTTTRAGTTT-3'). All samples were sent to the Majorbio Bio-pharm Technology Co., Ltd (Shanghai, China) for high throughput sequencing and qPCR, and each sample was detected in triplicate. The data were analyzed on the free online platform of the Majorbio Cloud Platform (www.Majorbio.com), and the similarity search was executed in the National Center for Biotechnology Information database (http://www.ncbi.nlm.nih.gov).

2.4 Rice seedling cultivation

After surface disinfection of rice seeds with 70% (v/v) EtOH and 5% (w/v) NaClO solution, the seeds were washed multiple times with deionized water until no chemical residues remained and placed in moist petri dishes for germination. Seed germination was held at 25 ± 2 °C and 18/6 h light/dark cycle in a light incubator. The experiment was halted on the fifth day, and rice seedlings with similar germination growth were selected for the following rice seedling growth test. Seedlings were incubated in an incubator at 25 °C with 18/6 h light/dark cycle for 21 days. AFA and water were regularly supplemented during this period to maintain the suitable acidic growth environment for rice seedlings.

The feasibility of AS for agricultural production was verified through rice plant index measurements. Germinationrate (%) was calculated by counting the number of rice seedlings at the sowing 5 d with reference to previous study. Finally, rice seedlings were recorded after 21 days of seed sowing and subsequently when plants were harvested. Seedlings were washed with deionized water and harvested to measure height (above/below ground plant parts). The dry biomass of rice seedlings was calculated after drying at 50 °C for about 12 h.

2.5 Characterization

The crystalline structures were identified by powder X-ray diffraction (XRD, Miniflex600, Japan Rigaku Corporation, Japan). Nitrogen adsorption–desorption isotherms were used to detect surface area and porosity analyzer (ASAP 2020 HD88, Micromeritics, USA). The surface functional groups were measured on an fourier transform infrared spectroscopy (FTIR, Nicolet iS50, Thermo Fisher Scientific, USA). The morphologies and surface element composition were tested by scanning electron microscopy (SEM, SUPRA 55 SAPPHIRE, Carl Zeiss, Germany) equipped with mapping (550i, IXRF Systems, Inc). The macropore structures of ABS and AS were investigated by high-resolution X-ray tomography and related data analysis (CT, FF20CT, YXLON International GmbH, Germany).

2.6 Statistics

Tests of homogeneity of variance were conducted, and separate one-way ANOVAs were performed to test for differences in treatments. Least significant difference (LSD) was used to make post-hoc comparisons between different treatments. Differences were considered significant at $p < 0.05$. Statistical analyses were conducted using SPSS 19.0 software. Figures were created using Origin 2016 and GraphPad Prism 9. Three or more replicates of experimental data were used for all error analyses.

3 Results and discussion

3.1 Component characteristics of anthropogenic soil

To define an optimal soil component through environmental engineering approach is difficult, which mainly involves nutrient indicator regulation, the hard-to-control arrangement of minerals and organic matter, and more. Classical synthetic humus formation was reactively auto-neutralizing during the hydrothermal humification reaction stages (Yang et al. 2019a; Wang et al. 2020). While in this study, the hydrothermal conversion reaction was chosen to go through a hydrothermal humidification-hydrothermal carbonization (HTH-HTC) process, where the length of the hydrothermal humification reaction was controlled by restricting the amount of base, while the acidic hydrothermal carbonization dominated the reaction at the end. With alkaline digestion of the biomass, sugars were first decomposed into the hydroxy- and keto-acids, until the pH in the reaction dropped to acidic values, and then the number of carboxylic acids was set. Condensation continued, involving a majority of the as-formed organic acids and phenols, and the pH of the solution dropped further. The degraded fragments under went dehydration, polymerization, aromatization, and decarboxylation reactions, creating the hydrochar (Zhuang et al. 2019; Cao et al. 2021). The final product had an acidic pH of 4.85 (ABS-15:1) (Table S2), as it facilitated the effective nutrient uptake and prevention of wilt diseases for acid-loving rice seedlings. That was itentional, as usually mineral acids were added, and the as-created orgnic acids are degradable and increased sustainability already in this first step. Morphologies of the original weak mineral soil and the as-built artificial black soil derived from conjugation with hydrothermal carbon species were revealed by SEM images (Fig. S1). The surface of the weak soil particles was smooth and showed

sheet-like fractures, while the as-prepared ABS mainly consisted of "cobble-like" particles with visible particle–particle glueing and adherent hydrochar particles, leading to great increase in the content of soil organic matter (from 3.16 ± 0.24% in weak soil to 19.49 ± 1.40% in ABS) and soil organic carbon (from 0.76 ± 0.22 in weak soil to 13.61 ± 1.18% in ABS). An initial approximation to determine potential mineralogical variations was done with XRD analysis. As presented in Fig. S2, for weak soil and artificial black soil samples, the locations of the dominant diffraction peaks match, namely at 20.85°, 26.64°, 36.54°, 39.46°, 42.45°, 50.14°, 59.96°, and 68.14°, respectively, which could be attributed to SiO_2 (PDF#98–000-0369). Some other corresponding peaks might be caused by either carbonates or silicates, such as $CaCO_3$, $Ca_2(SiO_4)$, $CaMg(Si_2O_6)$, $MgSiO_3$, $Mg_2(Si_2O_6)$, Mg_2SiO_4, $Mg(SiO_3)$ and $Mg(SiO_3)$ (Yang et al. 2020). FTIR spectroscopy (Fig. S3) revealed that ABS samples showed emerging characteristic peaks at 2934 cm^{-1}, 2856 cm^{-1}, and 1698 cm^{-1} when compared to weak soil. 2856 cm^{-1} and 2934 cm^{-1} modes were generally attributed to the aliphatic stretching vibrations of -CH_3 and -CH_2, and peaks located at about 1698 cm^{-1} were caused by the stretching vibration of C=O bonds of -COOH and ketones (Yang et al. 2019a), indicating that as-formed humic matters produced from hydrothermal humification were conjugated onto the primary soil particles. The absorption band at 3400 cm^{-1} was related to ν_{OH} stretch of phenolic and hydroxyl C groups (Ndzelu et al. 2021). The absorption peaks near 530 cm^{-1} exhibited the bending vibrations of Si–O-Al and Si–O-Mg bonds, and that near 460 cm^{-1} belonged to Si–O-Si. Apparently, the original soil mineral composition and surface functional groups were basically maintained in the neighbourhood of the-strongly interactive humic acids. N_2 adsorption–desorption isotherms (Fig. S4) described that both samples displayed a Type IV(a) isotherm with hysteresis loop of Type H4, according to the classification of the IUPAC, which pointed to the existence of micro-mesoporous structure (Wang et al. 2022). The pore size distribution displayed a considerable increase in pore volume and pore size for ABS-15:1 (0.041 cm^3/g and 7.24 nm) compared with that for weak soil (0.031 cm^3/g and 4.57 nm) (Table S4). Even so, ABS-15:1 showed the lower specific surface area, suggesting the filling of original mineral micropores by organic species. The above findings revealed that an artificial black soil concentrate or masterbatch with a physical and chemical structure similar to natural soil had been produced, setting the chemical base for the further biological colonialization.

Fig. S5 and Fig. S6 show that straw is a necessary carbon source for the production of artificial black soil through hydrothermal humification-carbonization. The resulting mineral particles and hydrochar fractions of the artificial black soil have a higher content of soluble humic substances compared to the weak soil or the carbon-reinforced soil containing hydrochar (hydrothermal carbonization). It has been confirmed that the hydrothermal humification-carbonization process is similar to the natural soil-forming process. This process involves the generation of "carbon sinks" (artificial humic substance-mineral and artificial humic substance-hydrochar) through polymerisation or abiotic self-assembly, as well as the continuous dissociation of soluble humic substances, rather than direct exogenous carbon recharge and carbonaceous pyrolysis processes (Yang et al. 2020, 2019a, 2023). This is the key to the upgrade of anthropogenic soil properties, especially agronomic properties, with artificial black soil as the functional fraction.

To make a better distinction, artificial black soil directly obtained through hydrothermal humification-hydrothermal carbonization was recorded as ABS, after that, artificial black soil was mixed with the weak soil in a certain ratio (10%, 30%, and 50% and incubated for a certain period of time for construction of anthropogenic soil, that is, the original weak soil was recorded as CK as a control experiment, and the other mixtures were recorded as AS-10, AS-30, and AS-50 according to the adulteration ratio in turn. After 30-day soil incubation with a dose of healthy soil microbiome and regular watering, anthropogenic soil gradually transitioned in appearance from yellow (original weak soil) to brown, dark brown, and black-like soil colour, with time and as the proportion of ABS addition increased (Fig. 2a). This implied that basic physicochemical properties and composition of anthropogenic soil significantly changed.

Soil organic matter content increased from 3.48 ± 0.22% (CK) to 4.68 ± 0.17% (AS-10), 8.69 ± 0.32% (AS-30), and 11.53 ± 0.42% (AS-50), and soil organic carbon content increased from 0.83 ± 0.18 (CK) to 1.99 ± 0.21 (AS-10), 5.02 ± 0.15 (AS-30), and 7.21 ± 0.09 (AS-50) (Fig. 2b, c). This was attributed to the direct carbon intakes from HTH-HTC, but also significantly to the biologically amplified carbon sequestration effect of AHS that had been evidenced in our previous studies (Tang et al. 2021, 2022).

The empirical critical values of soil organic carbon concentration were universally perceived to be 2%, below which soil microbial diversity and crop yield were linearly reduced, and organic carbon content in AS was close to or above 2%, which was necessary for seedling substrates without the secondary incorporation of boosters (Stockmann et al. 2015). It had been reported that, unlike biochar, the level of available phosphorus may somewhat "regress" with hydrochar application for pH effects and physical adsorption

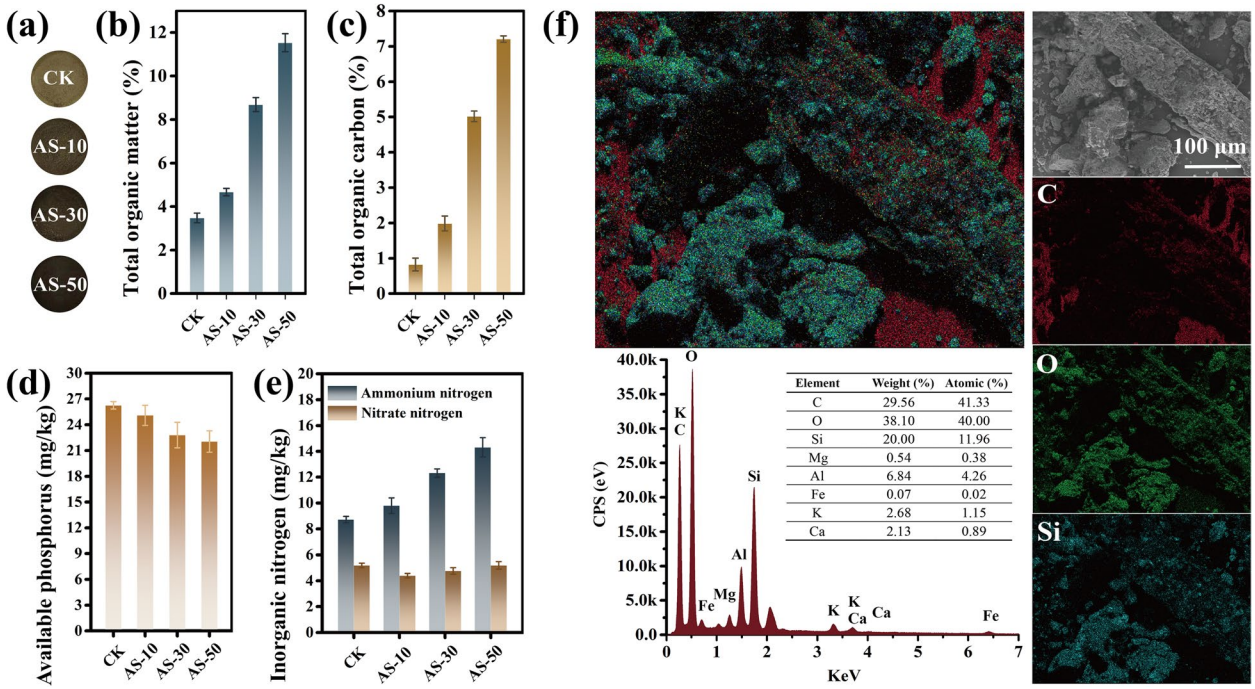

Fig. 2 Physical indicators of the reconstructed anthropogenic soil. The appearance (**a**), total organic matter (**b**), total organic carbon (**c**), available phosphorus (**d**), and inorganic nitrogen (nitrate and ammonium nitrogen) (**e**) of CK, AS-10, AS-30, and AS-50 samples; and (**f**) SEM-mapping of AS-50

phenomena (Tarf et al. 2022; Cervera-Mata et al. 2021). There was a slight decreasing trend of available phosphorus content in AS-10 ~ 50 that contained hydrochar, decreasing from 26.26 ± 0.42426 mg/kg (control group) to 25.10 ± 1.16 mg/kg (AS-10), 22.81 ± 1.48 mg/kg (AS-30), 22.06 ± 1.24 mg/kg (AS-50) (Fig. 2d), which pointed to solubilized phosphate escaping into bulk liquid product owing to poor soil mineral and biomass fraction structure eroded during hydrothermal humification-carbonation, as previously demonstrated, as proven previously (Yang et al. 2019b; Du et al. 2020). And related studies had shown that the increase in organic carbon content may also result in available phosphorus content reduction, i.e., microbial activity effect (Wei et al. 2021). What was exciting is that, available phosphorus level in anthropogenic soil was sufficient, as anthropogenic soil already contained the critical fertility level (20 mg/kg) for most field crops, and artificial humic substances will be returned to the anthropogenic soil as "acid regulators" and "nutrients" as needed during the rice seedling planting period, further compensating for the loss of available phosphorus. Nitrate and ammonium nitrogen were the main inorganic nitrogen species in the soil. As observed, nitrate nitrogen in AS-10 ~ 50 gradually increased to reach the same levels as CK (5.19 ± 0.18 mg/kg), while ammonium nitrogen significantly increased from 8.73 ± 0.25 (CK) to 9.80 ± 0.60 mg/kg, 12.32 ± 0.32 mg/kg, and 14.32 ± 0.75 mg/kg (Fig. 2e), suggesting that anthropogenic soils create ammonia by metabolic activities, well above the previously contained nitrate content of the weak soil. HTH-HTC derivatives, through chemical and biological pathways, played the decisive contribution for ammonium nitrogen fixation, forming the more stable NH_4^+-artificial humic structure through complexation, and furthermore enhancing microbial nitrogen fixation activity (Xu et al. 2021, 2019), also as demonstrated later in this paper. Morphologies of anthropogenic soil obtained by mixing the masterbatch with the poor soil could be clearly followed by SEM images, which was similar to ABS sample, as shown in Fig. S7, S8. Results of SEM-Mapping analysis, typified with AS-50, showed that the surface of sample was dominated by C (29.56 wt%, 41.33 at%), O (38.10 wt%, 40.00 at%), and Si (20.00 wt%, 11.96 at%) elements (Fig. 2f), and small amounts of Mg, Al, Fe, K, and Ca elements (Fig. S9). The above results already suggested that the reconstructed seedling soils had superior properties and high fertility, attributed to reconstruction of a humic layer, leading to refined soil texture and available nutrients.

3.2 Optimization of anthropogenic soil mechanical structure

Soil architecture, which has an intimate correlation to soil ecological functions, surface water and energy fluxes, and plant growth. Bulk density (BD) and water holding capacity (WHC), as soil structure parameters, are the first simple measures to quantify the hydrological water transfer function of the presented synthetic soil (Verheijen et al. 2019). Figure 3a-d presents the changes in maximum WHC and BD values in CK and AS samples. Specifically, there was a significant increase in gravimetric maximum WHC for AS-30 (69.72 ± 1.40%) and AS-50 (80.03 ± 1.97%) as compared to CK (53.72 ± 2.97%) and AS-10 (56.28 ± 1.46%) (Fig. 3a). The BD of AS visibly decreased from 1.05 ± 0.033 g/cm^3 (CK) to 1.04 ± 0.026 g/cm^3 (AS-10), 0.89 ± 0.013 g/cm^3 (AS-30), and 0.804 ± 0.007 g/cm^3 (AS-50). This was also pointing to the ability of carbon species to stabilize interstitial pores, which in return improved gas transport through an interconnected porous soil texture.

From Fig. 3c, d, it could be concluded that the percentage of ABS in AS was the main factor affecting the maximum WHC and minimal BD. This demonstrated that ABS did not only effectively enhance the nutrient availability but also regulated the water-holding and water-retention capacity of AS, which was significantly related to crop growth and soil structure optimization.

The pore system was analysed by BET (on the nanoscale) and CT scanning techniques (on the micro- to macroscale). As shown in Fig. S10 and Table S5, the specific surface area and pore volume of CK and AS-10 ~ 50 gradually decreased from 39.3419 m^2/g (CK) to 35.30 m^2/g (AS-10), 27.67 m^2/g (AS-30), 17.67 m^2/g (AS-50), and from 0.041 to 0.038 cm^3/g (AS-10), 0.036 cm^3/g (AS-30), and 0.031 cm^3/g (AS-50), respectively. The accessible pore size tended to significantly increase at the

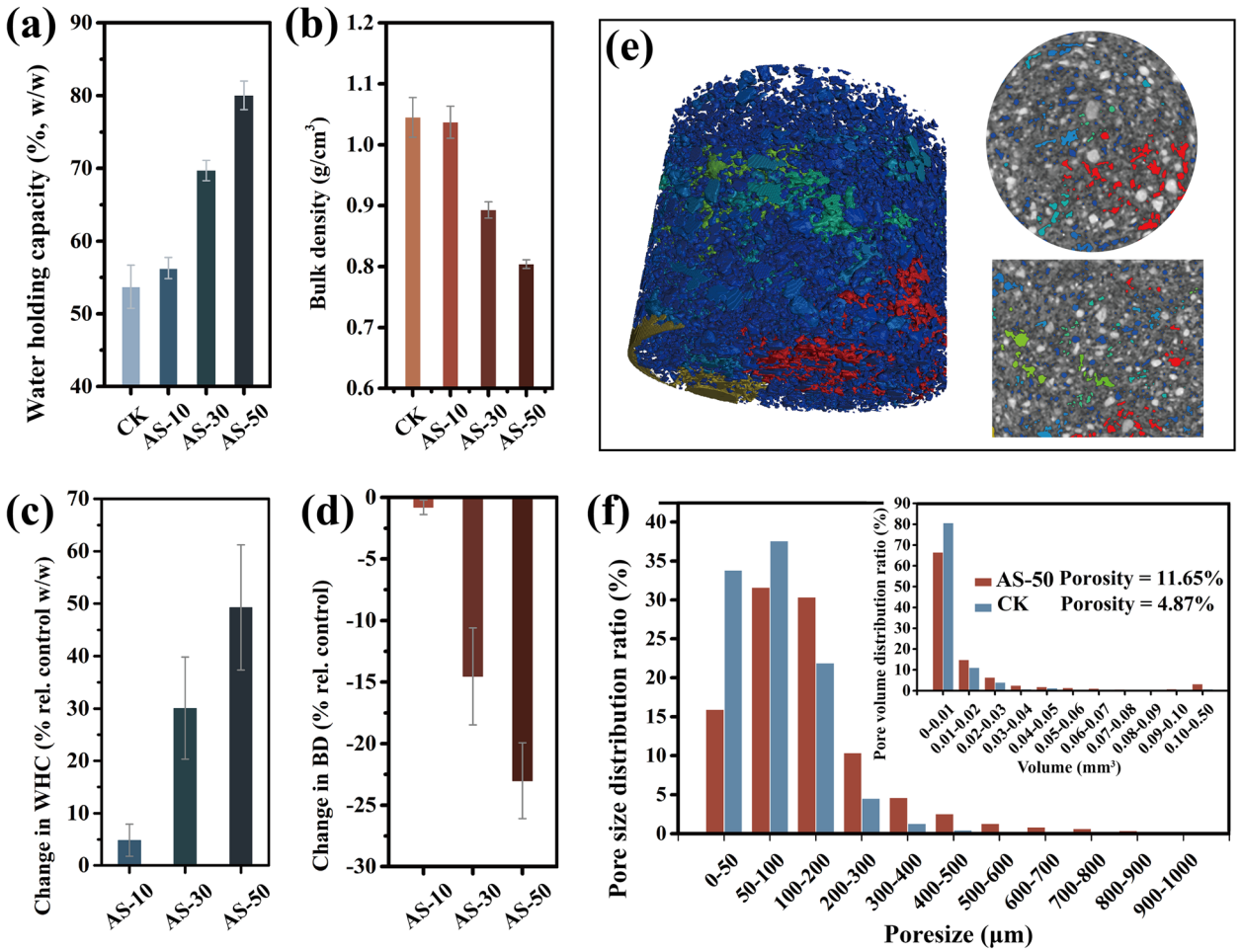

Fig. 3 Structural indicators of the reconstructed anthropogenic soil. The gravimetric maximum water holding capacity (**a**), bulk density (**b**), changes in gravimetric maximum water holding capacity (**c**), and changes in bulk density (**d**) of control group CK, AS-10, AS-30, and AS-50; (**e**) Visualization of the AS-50 cores; (**f**) Pore diameter and volume distribution of AS-50 cores

nanoscale, especially for AS-30 (4.86 nm) and AS-50 (5.98 nm), this, however, just reflected the organic filling of smaller micropores.

As shown in Fig. S10, CK and AS-50 samples were selected for further CT characterization and related analysis. The pores of AS-50 were relatively uniform and well-developed, while those of CK are mostly at the lower end of accessibility. There were also obvious discrepancies in image grayscale, with a lower density of AS-50 than CK. Specifically, the porosity of AS-50 (11.65%) was found much higher than that of CK (4.87%), especially in the proportion of larger pore diameters and pore volumes of 100–1000 μm. Similarly, the proportion of pore volumes in the range of 0.02–0.5 mm^3 was larger than that of CK (Fig. 3e, f). The above results indicated that structure of anthropogenic soil, especially the macropore structure, had been effectively improved, presumably by interconnecting primary particles to humic-bridged aggregated which then could not densely pack, which in turn regulated the soil habitat function.

3.3 Reconstruction of microbial systems in anthropogenic soil

To monitor the assumed development of bacterial and fungal communities in a series of anthropogenic seedling soils after 30-day incubation, the samples were also analyzed based on 16S rRNA and ITS high-throughput sequencing techniques. Veen graph results showed that OTU numbers of soil bacteria and fungi in the control and each experimental groups ranged from 918 to 482 and 401 to 231, respectively, at the 97% sequence similarity level, with the highest number of OTUs in the CK group, while those in AS-10, AS-30, and AS-50 treatments decreased in OUT number with the increased of added AS (Fig. S12). The structural changes of bacterial and fungal communities within the experimental groups were visualized through α diversity analysis (Fig. 4a, b). The bacterial community richness and diversity of AS-10 showed no significant difference compared to CK ($p > 0.05$) and was even slightly higher. The bacterial community richness of AS-50 was significantly lower than those in other experimental groups ($p < 0.05$), and the diversity in AS-50 was also significantly lower than that in the AS-10 experimental group ($p < 0.05$). The changes of the soil fungal α-diversity were shown in Fig. 4b, and there was no significant difference ($p < 0.05$) for fungal diversity among various experimental groups. Species richness in AS-50 was significantly lower than those in AS-10 and AS-30 ($P < 0.05$). The taxonomic composition of bacteria in the soil was dominated by three phyla, following the order of *Proteobacteria*, *Actinobacteria*, and *Bacteroidota* (Fig. 4c, Table S6; Zou et al. 2018). Compared with the weak soil, the relative abundance of *Proteobacteria* in AS significantly increased (77.71 ± 2.11% ~ 86.67 ± 3.00% *versus* 58.22 ± 2.11% in CK), whereas the relative abundance of *Actinobacteria* (9.65 ± 0.89% ~ 14.92 ± 0.71% *versus* 24.69 ± 3.63% in CK) and *Bacteroidetes* (0.97 ± 0.45% ~ 2.05 ± 0.81% *versus* 5.73 ± 1.56% in CK) significantly decreased. The result implicated that the available nutrients in AS (especially AS-30 and AS-50) may preferentially support the growth of coprophilic bacteria (such as *Proteobacteria*) (Zou et al. 2018; Dai et al. 2018). AS provided a favorable nutritional habitat for bacterial metabolism (Yang et al. 2021b). For fungi, the leading phylum composed of AS was *Ascomycota* (96.87 ± 1.32% ~ 99.23 ± 3.87%), which exceeded the percentage of weak soil. *Bacteroidota* and *Glomeromycota* showed decreasing trends in AS, when compared to weak soil (Fig. 4d, Table S7). *Ascomycota* contributed to the degradation of organic substrates, and the highest abundances were found in AS-30 (98.65 ± 6.81%) and AS-50 (99.23 ± 3.87%) (Yang et al. 2021b). Ascomycota were also "sporeshooters" and multiplied asexually very rapidly.

On the other hand, the composition and relative abundance of bacteria and fungi in AS at the OTU level significantly changed, and excitingly, some microorganisms that increased soil nutrients or promoted crop growth appeared or increased in proportion. OTU995, which occurred in AS, matched *Caballeronia calidae*, a plant growth promoter (Kirui et al. 2022). Besides, ammonium nitrogen was as-known the most sensitive nitrogen fraction made by nitrogen-fixing microorganisms, and worth noting, *Herbaspirillum frisingense* (OUT114), a nitrogen-fixing bacterial species, showed favored growth in AS, thus a posteriori explaining the increased ammonia content (Xu et al. 2019; Kirchhof et al. 2001). Also, OTU486, *Humicola*, a beneficial fungus, was more abundant in AS (AS-30 > AS-50 > AS-10) as compared to CK (Lang et al. 2012). The above results indicated that microbial communities in anthropogenic soil had been reconstituted, and the pace and capacity of reconstruction were obviously related to the amount of ABS. Especially the fungal species α diversity could be rapidly built up in a short time (30 days). This can be achieved through the "grafting" of microbial communities from weak soil to "diluted" anthropogenic soil. At the same time, some microorganisms that facilitate plant growth increased in abundance or even firstly emerged above their detection threshold.

3.4 Biometric attributes of rice seedlings in anthropogenic soil -based substrates

This rich microbial community, together with higher amounts of soluble P and ammonia created by bacterial operations, will stimulate plant growth. In Fig. 5a, b and Fig. S13, a significant promotion effect on seed

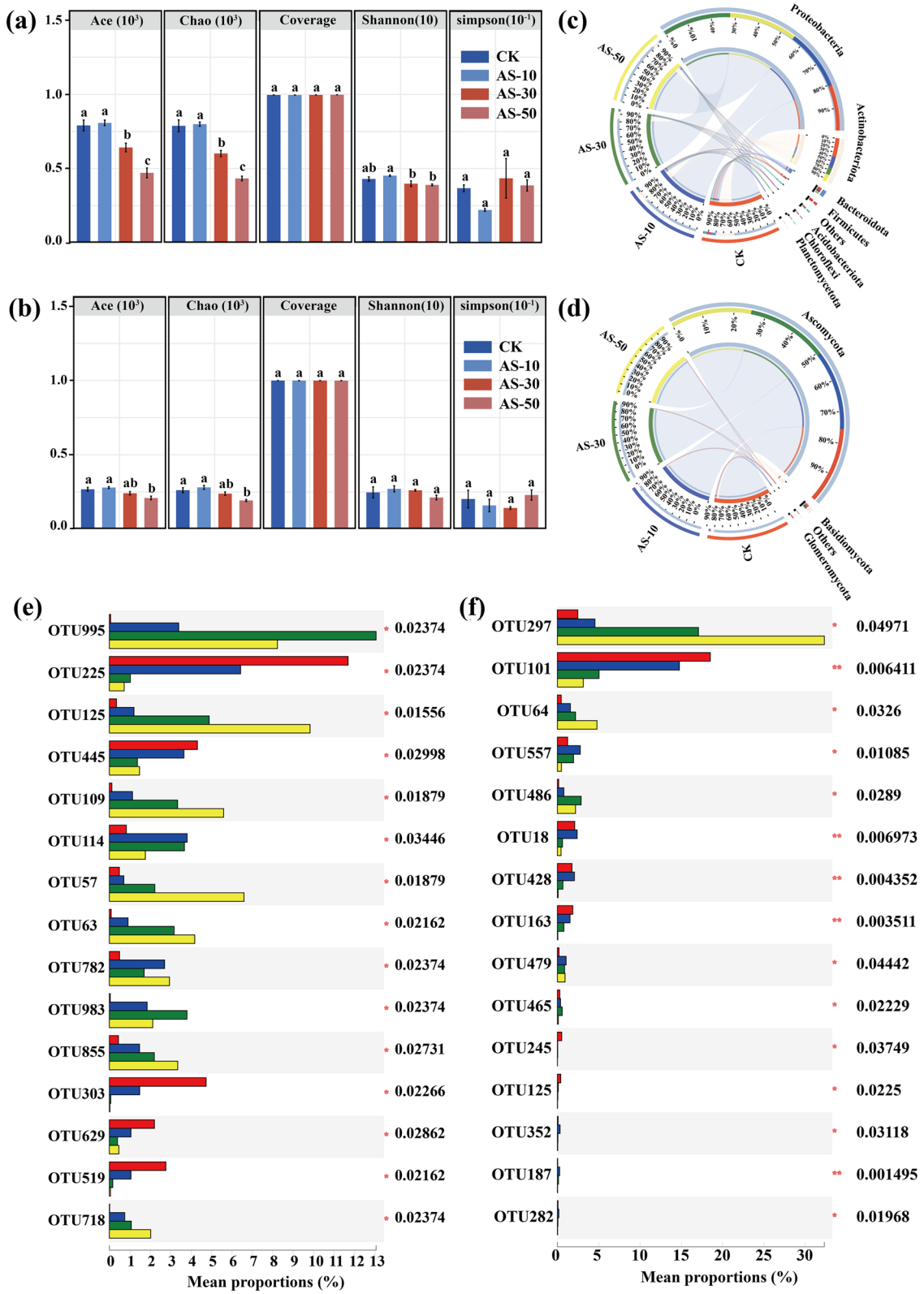

Fig. 4 Microbial indicators of reconstructed anthropogenic soil. The bacterial and fungal species composition diversity (**a**-**b**), species composition at the phylum level (**c**-**d**), one-way ANOVA for species composition at the OTU level (**e**–**f**) of CK, AS-10, AS-30, and AS-50 samples

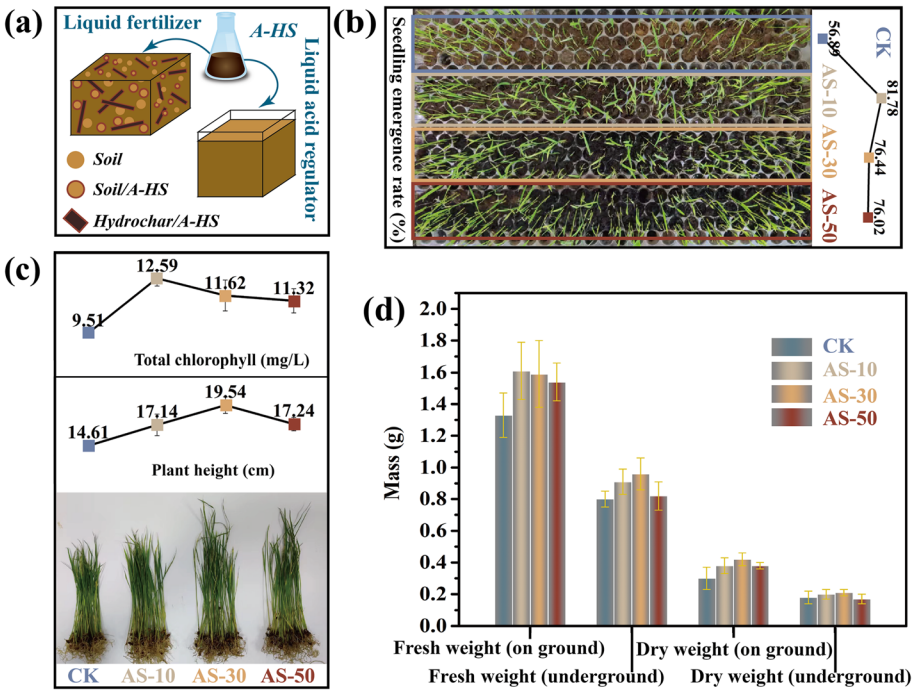

Fig. 5 Rice seedling growth indicators of reconstructed anthropogenic soil. (**a**) Scheme of the construction process of SS-10 ~ 50; (**b**) Seedling germination rate in CK and SS-10 ~ 50; (**c**) Rice seedlings of plant growth, plant height, and total chlorophyll content in CK and SS-10 ~ 50; (**d**) Dry weight/fresh weight of above/below ground portion of rice seedlings

germination and seeding growth could be quantified in the diverse engineering soils. Note that in the present set of experiments, no mineral acids, fertilizer, or other chemical boosters were added. The experiments aimed to replicate natural conditions as closely as possible, except for using an engineered soil. ABS introduction could improve seed germination from 56.89% (CK) to 81.78%, 76.44%, and 76.02% in all three treatment groups (AS-10, AS-30, and AS-50). On top, noticeable increase of seedling height and total chlorophyll content were observed for seedlings grown in anthropogenic seedling soils. Specifically, the average seedling height was 14.61 ± 0.64 cm in CK, and increased to 17.14 ± 1.32, 19.54 ± 1.01, and 17.24 ± 0.82 cm in AS-10, AS-30, and AS-50 samples, respectively (Fig. 5c). Total chlorophyll content of seedlings grown in control group was 9.51 ± 0.22 mg/L, while those in experimental AS-10, AS-30 and AS-50 samples increased to 12.59 ± 0.44, 11.62 ± 0.87 and 11.32 ± 0.68 mg/L, respectively. Dry/fresh weights of above/below ground parts of rice seedlings were also measured to further evaluate the actual production effects in AS groups (Fig. 5d). Broadly corresponding to the above results, the fresh weight of above/below ground parts in AS-10, AS-30 and AS-50 group was increased to 1.61 ± 0.18/0.91 ± 0.08 g, 1.59 ± 0.21/0.96 ± 0.10 g, and 1.54 ± 0.12/0.82 ± 0.09 g, respectively, as compared to 1.33 ± 0.14 / 0.80 ± 0.05 g for seedlings grown in CK group. Compared to dry weight of above/below ground parts of 0.30 ± 0.07 / 0.18 ± 0.04 g for seedlings grown in CK group, the weights were 0.38 ± 0.05/0.20 ± 0.03 g, 0.42 ± 0.04/0.21 ± 0.02 g, and 0.38 ± 0.02/0.17 ± 0.03 g for AS-10, AS-30 and AS-50 groups, respectively.

Anthropogenic soil promotes better biometric attributes, which reply both on superior physical–chemical functionality and soil microbial activity, such as an remarkable increase in ammonium nitrogen, generated by identified nitrogen fixing bacteria. Ammonium ions were actively taken up by the root system through ammonium transport proteins and then assimilated as the amide residue of glutamine (Gln) through the reaction of glutamine synthetase (GS) in the root (Tabuchi et al. 2007). This matched with the results of previous study that the main source of inorganic nitrogen for rice plants grown in rice soils was ammonium nitrogen from the soil (Tabuchi et al. 2007; Luo et al. 2022). Furthermore, correlation analysis revealed that soil ammonium nitrogen concentration, rather than pH value or nitrate nitrogen concentration, determined the composition of the soil bacterial community (Nie et al. 2018). The biochemical promotion of rice seedlings was regulated by the multiple constituent-structure of anthropogenic soil rather than a single nutrient or water supply/stress

mechanism. Anthropogenic soil promotes better biometric attributes, which reply both on superior physical–chemical functionality and soil microbial activity, such as a remarkable increase in ammonium nitrogen, generated by identified nitrogen fixing bacteria. This was verified through the fact that a composition variation of anthropogenic soils (AS-10, AS-30, and AS-50) changes germination rate, plant height, and total chlorophyll content. This was on top validated through application of AS containing the highest organic carbon fraction (AS-50) in large-scale practical agricultural production (a high carbon content was chosen to allow high dilution after application, typical for freeland experiments). Fig. S14 showed that AS promoted the growth of rice seedlings (30 days) and rice roots (150 days), as well as increased the water stability of soil aggregates. This AS and the coupled microbiome delivered with the seedlings to the farm land and co-applied with the seedling, which ensures the "in-situ" nutrient supply for rice seedlings during the following periods. AS was thereby the source of sustainable agriculture for providing the organic matter, mineral elements and others necessary inputs to top soil.

4 Conclusions

The objective of this study was to explore an artificial black soil made by hydrothermal process based on biomass side products for the amendment of weak mineral soil and the promotion of the growth of rice seedlings. Anthropogenic soil thereby replaces peat or other refined seedling soils and makes their acidification by sulfuric acid superfluous, i.e., it clearly contributes to a more sustainable agriculture, as artificial fulvic or other organic acids are food for microorganisms and vanish afterwards (in contrast to sulfuric acid, solid acids, and commercial preparations, which are added into agricultural soils but do not degrade). Anthropogenic soil makes mixing of this conjugated mineral-carbon primer and standard soil shown a remarkable decrease in bulk density, along with significant increases in total organic matter ($4.68 \pm 0.17\% \sim 11.53 \pm 0.42\%$), total organic carbon ($1.99 \pm 0.21\% \sim 7.21 \pm 0.09\%$), ammonium nitrogen ($9.80 \pm 0.60$ mg/kg $\sim 14.32 \pm 0.75$ mg/kg), macropore porosity, and macropore diameter/volume. The results suggested that AS-30 possessed excellent physicochemical and agronomic properties, which can be used as an essential reference for subsequent studies on constructing anthropogenic soils. Promotion of plant growth was also clearly observed, while metagenomics data illustrated the quick recovery of the microbial systems, especially the abundance of fungi, but also the occurrence and growth of plant supporting bacteria. As such, a fertile soil environment could be reconstituted in only 4 weeks, while natural recovery would take much longer. This simple and universal "terraforming" technology (or refined versions of it) will not only help to bring agriculture into a Moon or Mars colony, but might also be necessary to sustain human life on Earth.

Abbreviations

ABS	Artificial black soil
HTH-HTC	Hydrothermal humification hydrothermal carbonization
AS	Anthropogenic soil
AFA	Artificial fulvic acid
SOC	Organic carbon
BD	Bulk density
WHC	Water holding capacity
XRD	Powder X-ray diffraction
FTIR	Fourier transform infrared spectroscopy
SEM	Scanning electron microscopy
CT	High-resolution X-ray tomography

Supplementary Information

The online version contains supplementary material available at https://doi.org/10.1007/s44246-024-00127-y.

Additional file 1.

Acknowledgements
Not applicable.

Author's contributions
All authors contributed to the study conception and design. Material preparation was performed by Yibo Lan, Fan Yang and Markus Antonietti. Data collection was performed by Ronghui Li, Qiang Fu, Kui Cheng and Zhuqing Liu. Analysis was performed by Yibo Lan, Markus Antonietti and Zhuqing Liu. The first draft of the manuscript was written by Yibo Lan and Fan Yang. All authors commented on previous versions of the manuscript. All authors read and approved the final manuscript.

Funding
This work is supported by the Outstanding Youth Project of Heilongjiang Province (JQ2021D001), National Key Research and Development Program of China (2022YFD1500100), National Natural Science Foundation of China (52279034).

Availability of data and materials
The datasets used or analyzed during the current study are available from the corresponding author on reasonable request.

Declarations

Competing interests
The authors have no relevant financial or non-financial interests to disclose.

Author details
[1]School of Water Conservancy and Civil Engineering, Northeast Agricultural University, Harbin 150030, China. [2]International Cooperation Joint Laboratory of Health in Cold Region Black Soil Habitat of the Ministry of Education, Harbin 150030, China. [3]College of Engineering, Northeast Agricultural University, Harbin 150030, China. [4]Max Planck Institute of Colloids and Interfaces Department of Colloid Chemistry, 14476 Potsdam, Germany.

Received: 4 November 2023 Revised: 1 April 2024 Accepted: 8 April 2024
Published online: 06 May 2024

References

Arcurs C (2017) Safeguarding Our Soils Nat Commun 8:2. https://doi.org/10.1038/s41467-017-02070-6

Cao Y, He MJ, Dutta S, Luo G, Zhang SC, Tsang DCW (2021) Hydrothermal carbonization and liquefaction for sustainable production of hydrochar and aromatics. Renew Sust Energ Rev 152:18. https://doi.org/10.1016/j.rser.2021.111722

Cervera-Mata A, Lara L, Fernandez-Arteaga A, Rufian-Henares JA, Delgado G (2021) Washed hydrochar from spent coffee grounds: A second generation of coffee residues. Evaluation as Organic Amendment Waste Manage 120:322–329. https://doi.org/10.1016/j.wasman.2020.11.041

Chang RX, Guo QY, Pandey P, Li YM, Chen Q, Sun Y (2021) Pretreatment by composting increased the utilization proportion of pig manure biogas digestate and improved the seedling substrate quality. Waste Manage 129:47–53. https://doi.org/10.1016/j.wasman.2021.05.010

Chen XJ, Zhang JH, Lin QM, Li GT, Zhao XR (2022) Dispose of Chinese cabbage waste via hydrothermal carbonization: hydrochar characterization and its potential as a soil amendment. Environ Sci Pollut Res 30(2):4592–4602. https://doi.org/10.1007/s11356-022-22359-4

Coban O, De Deyn GB, van der Ploeg M (2022) Soil microbiota as game-changers in restoration of degraded lands. Science 375(6584):990–1000. https://doi.org/10.1126/science.abe0725

Dai ZM, Su WQ, Chen HH, Barberan A, Zhao HC, Yu MJ, Yu L, Brookes PC, Schadt CW, Chang SX, Xu JM (2018) Long-term nitrogen fertilization decreases bacterial diversity and favors the growth of Actinobacteria and Proteobacteria in agro-ecosystems across the globe. Glob Change Biol 24(8):3452–3461. https://doi.org/10.1111/gcb.14163

Du Q, Zhang SS, Antonietti M, Yang F (2020) Sustainable Leaching Process of Phosphates from Animal Bones To Alleviate the World Phosphate Crisis. ACS Sustain Chem Eng 8(26):9775–9782. https://doi.org/10.1021/acssuschemeng.0c02233

Janzen HH, Janzen DW, Gregorich EG (2021) The "soil health" metaphor: Illuminating or illusory? Soil Biol Biochem 159:10. https://doi.org/10.1016/j.soilbio.2021.108167

Kirchhof G, Eckert B, Stoffels M, Baldani JI, Reis VM, Hartmann A (2001) Herbaspirillum frisingense sp. nov., a new nitrogen-fixing bacterial species that occurs in C4-fibre plants. Int J Syst Evol Micr 51(Pt 1):157–168. https://doi.org/10.1099/00207713-51-1-157

Kirui CK, Njeru EM, Runo S (2022) Diversity and Phosphate Solubilization Efficiency of Phosphate Solubilizing Bacteria Isolated from Semi-Arid Agroecosystems of Eastern Kenya. Microbiol Insights 15:11786361221088992. https://doi.org/10.1177/11786361221088991

Kopittke PM, Menzies NW, Wang P, McKenna BA, Lombi E (2019) Soil and the intensification of agriculture for global food security. Environ Int 132:8. https://doi.org/10.1016/j.envint.2019.105078

Lang JJ, Hu J, Ran W, Xu YC, Shen QR (2012) Control of cotton Verticillium wilt and fungal diversity of rhizosphere soils by bio-organic fertilizer. Biol Fertil Soils 48(2):191–203. https://doi.org/10.1007/s00374-011-0617-6

Luo L, Zhu M, Jia LT, Xie YM, Wang ZN, Xuan W (2022) Ammonium transporters cooperatively regulate rice crown root formation responding to ammonium nitrogen. J Exp Bot 73(11):3671–3685. https://doi.org/10.1093/jxb/erac059

Meng XY, Wang QP, Lv Z, Cai YF, Zhu MC, Li JL, Ma XG, Cui ZJ, Ren LH (2022) Novel seedling substrate made by different types of biogas residues: Feasibility, carbon emission reduction and economic benefit potential. Ind Crop Prod 184:12. https://doi.org/10.1016/j.indcrop.2022.115028

Ndzelu BS, Dou S, Zhang XW, Zhang YF, Ma R, Liu X (2021) Tillage effects on humus composition and humic acid structural characteristics in soil aggregate-size fractions. Soil Tillage Res 213:10. https://doi.org/10.1016/j.still.2021.105090

Nie YX, Wang MC, Zhang W, Ni Z, Hashidoko Y, Shen WJ (2018) Ammonium nitrogen content is a dominant predictor of bacterial community composition in an acidic forest soil with exogenous nitrogen enrichment. Sci Total Environ 624:407–415. https://doi.org/10.1016/j.scitotenv.2017.12.142

Richter DD (2021) A World Without Soil: The Past, Present, and Precarious Future of the Earth Beneath Our Feet. Science 374(6574):1452–1452. https://doi.org/10.1126/science.abm4765

Stockmann U, Padarian J, McBratney A, Minasny B, de Brogniez D, Montanarella L, Hong SY, Rawlins BG, Field DJ (2015) Global soil organic carbon assessment. Glob Food Secur-AgricPolicy 6:9–16. https://doi.org/10.1016/j.gfs.2015.07.001

Tabuchi M, Abiko T, Yamaya T (2007) Assimilation of ammonium ions and reutilization of nitrogen in rice (Oryza sativa L.). J Exp Bot 58(9):2319–2327. https://doi.org/10.1093/jxb/erm016

Tang CY, Li YL, Song JP, Antonietti M, Yang F (2021) Artificial humic substances improve microbial activity for binding CO2. iScience 24(6):14. https://doi.org/10.1016/j.isci.2021.102647

Tang CY, Cheng K, Liu BL, Antonietti M, Yang F (2022) Artificial humic acid facilitates biological carbon fixation under freezing-thawing conditions. Sci Total Environ. 849:157841

Tarf OJ, Akca MO, Donar YO, Bilge S, Turgay OC, Sinag A (2022) The short-term effects of pyro-and hydrochars derived from different organic wastes on some soil properties. Biomass Convers Biorefinery 12(1):129–139. https://doi.org/10.1007/s13399-021-01282-7

Tautges NE, Chiartas JL, Gaudin ACM, O'Geen AT, Herrera I, Scow KM (2019) Deep soil inventories reveal that impacts of cover crops and compost on soil carbon sequestration differ in surface and subsurface soils. Glob Change Biol 25(11):3753–3766. https://doi.org/10.1111/gcb.14762

Verheijen FGA, Zhuravel A, Silva FC, Amaro A, Ben-Hur M, Keizer JJ (2019) The influence of biochar particle size and concentration on bulk density and maximum water holding capacity of sandy vs sandy loam soil in a column experiment. Geoderma 347:194–202. https://doi.org/10.1016/j.geoderma.2019.03.044

Wall DH, Six J (2015) Give soils their due. Science 347(6223):695–695. https://doi.org/10.1126/science.aaa8493

Wang WJ, Wang Q, Zhou W, Xiao L, Wang HM, He XY (2018) Glomalin changes in urban-rural gradients and their possible associations with forest characteristics and soil properties in Harbin City, Northeastern China. J Environ Manage 224:225–234. https://doi.org/10.1016/j.jenvman.2018.07.047

Wang CQ, Zhang X, Sun RR, Cao YJ (2020) Neutralization of red mud using bio-acid generated by hydrothermal carbonization of waste biomass for potential soil application. J Clean Prod 271:9. https://doi.org/10.1016/j.jclepro.2020.122525

Wang G, Liang G, Xiao H, Qiu J, Liu H, Ma S, Komarneni S (2022) Immobilization mechanism of As, Mn, Pb and Zn ions in sulfide tailings by the addition of triethylenetetramine-montmorillonite nanocomposite. Chem Eng J 435:134817. https://doi.org/10.1016/j.cej.2022.134817

Wei YQ, Wang J, Chang RX, Zhan YB, Wei D, Zhang L, Chen Q (2021) Composting with biochar or woody peat addition reduces phosphorus bioavailability. Sci Total Environ 764:9. https://doi.org/10.1016/j.scitotenv.2020.142841

Xu YD, Wang T, Li H, Ren CJ, Chen JW, Yang GH, Han XH, Feng YZ, Ren GX, Wang XJ (2019) Variations of soil nitrogen-fixing microorganism communities and nitrogen fractions in a Robinia pseudoacacia chronosequence on the Loess Plateau of China. CATENA 174:316–323. https://doi.org/10.1016/j.catena.2018.11.009

Xu JC, Mohamed E, Li Q, Lu T, Yu HJ, Jiang WJ (2021) Effect of Humic Acid Addition on Buffering Capacity and Nutrient Storage Capacity of Soilless Substrates. Front Plant Sci 12:12. https://doi.org/10.3389/fpls.2021.644229

Yang F, Antonietti M (2020) The sleeping giant: A polymer View on humic matter in synthesis and applications. Prog Polym Sci 100:9. https://doi.org/10.1016/j.progpolymsci.2019.101182

Yang F, Zhang SS, Cheng K, Antonietti M (2019a) A hydrothermal process to turn waste biomass into artificial fulvic and humic acids for soil remediation. Sci Total Environ 686:1140–1151. https://doi.org/10.1016/j.scitotenv.2019.06.045

Yang F, Zhang SS, Song JP, Du Q, Li GX, Tarakina NV, Antonietti M (2019b) Synthetic Humic Acids Solubilize Otherwise Insoluble Phosphates to Improve Soil Fertility. Angew Chem-Int Edit 58(52):18813–18816. https://doi.org/10.1002/anie.201911060

Yang F, Zhang SS, Fu Q, Antonietti M (2020) Conjugation of artificial humic acids with inorganic soil matter to restore land for improved conservation of water and nutrients. Land Degrad Dev 31(7):884–893. https://doi.org/10.1002/ldr.3486

Yang F, Tang CY, Antonietti M (2021a) Natural and artificial humic substances to manage minerals, ions, water, and soil microorganisms. Chem Soc Rev 50(10):6221–6239. https://doi.org/10.1039/d0cs01363c

Yang Y, Tong YA, Liang LY, Li HC, Han WS (2021b) Dynamics of soil bacteria and fungi communities of dry land for 8 years with soil conservation management. J Environ Manage 299:10. https://doi.org/10.1016/j.jenvman.2021.113544

Yang F, Fu Q, Antonietti M (2023) Anthropogenic, Carbon-Reinforced Soil as a Living Engineered Material. Chem Rev. 123(5):2420–2435. https://doi.org/10.1021/acs.chemrev.2c00399

Zhuang XZ, Zhan H, Song YP, He C, Huang YQ, Yin XL, Wu CZ (2019) Insights into the evolution of chemical structures in lignocellulose and non-lignocellulose biowastes during hydrothermal carbonization (HTC). Fuel 236:960–974. https://doi.org/10.1016/j.fuel.2018.09.019

Zou Q, An WH, Wu C, Li WC, Fu AQ, Xiao RY, Chen HK, Xue SG (2018) Red mud-modified biochar reduces soil arsenic availability and changes bacterial composition. Environ Chem Lett 16(2):615–622. https://doi.org/10.1007/s10311-017-0688-1

Publisher's Note